Stereochemical Aspects of Enantiopure and Racemic Organolithium Aggregates Li_4Ar_4 {Ar = C_6H_4[CH(Me)NMe_2]-2}

Claudia M. P. Kronenburg,[a] Evelien Rijnberg,[a] Johann T. B. H. Jastrzebski,[a] Huub Kooijman,[b] Anthony L. Spek,[b] and Gerard van Koten*[b]

Dedicated to the memory of Dr. Ron Snaith and his great contribution to organolithium chemistry

Keywords: Lithiation / Lithium / Racemic compounds / Structure elucidation

The compounds (*R*)- and *rac*-[1-(dimethylamino)ethyl]benzene, (*R*)-**1** and *rac*-**1**, respectively, react quantitatively with *t*BuLi in a 1:1 molar ratio in pentane to give the corresponding (*R*)- and *rac*-[Li_4{C_6H_4[CH(Me)NMe_2]-2}$_4$], (*R*)-**2** and *rac*-**2**, respectively. The same reaction with *n*BuLi afforded a 1:1:1 aggregate of *n*BuLi, **2**, and **1** according to the results of quench experiments with H_2O and D_2O. The ^1H, ^{13}C, and ^7Li NMR spectra, as well as the single-crystal X-ray structure, reveal that (*R*)-**2** has a unique self-assembled tetranuclear structure of two diastereoisomeric dimeric units both in solution, in non-coordinating hydrocarbon solvents, and in the solid state. Detailed information about *rac*-**2**, which, in contrast to the high solubility of (*R*)-**2**, is essentially insoluble in hydrocarbon solvents, was provided by ^{13}C CP/MAS NMR spectra. We conclude that *rac*-**2** is a self-assembled tetranuclear aggregate comprising a combination of two dimeric units, but in this case they are derived from the (*R*)- and (*S*)-enantiomers, respectively.
(© Wiley-VCH Verlag GmbH & Co. KGaA, 69451 Weinheim, Germany, 2004)

Introduction

The use of organolithium reagents in chemical synthesis has increased enormously during the last 30 years.[1,2] Their relatively simple synthesis and high reactivity make organolithium compounds often more attractive reagents in organic synthesis than are the corresponding Grignard reagents. The most widely used organolithium compound, *n*BuLi, is currently applied to both laboratory-scale syntheses and large-scale industrial processes. Aryllithium compounds, especially *ortho*-lithiated ones, have proven to be important reagents in the synthesis of functionalized aromatic compounds and are of great interest to organic chemists.[3,4] Furthermore, they are frequently used in transmetallation reactions that lead to catalytically active organometallic complexes, e.g., aryl−platinum metal complexes[5] and related copper and zinc species.[6−11]

In general, organolithium species associate through their electron-deficient carbon−lithium bonds. The type of aggregation that these compounds undergo is governed by steric factors and the presence of heteroatom-containing donor groups, which can be either solvent molecules or inter- or intramolecularly coordinating substituents in the organic monoanion.[2,12] These inter- and intramolecular donor groups are known to affect the synthesis and reactivity of organolithium reagents.[13−17] For the synthesis of *ortho*-lithiated aryl compounds, direct lithiation is commonly used by hydrogen−lithium exchange (deprotonation) of the *ortho*-substituted arene with a suitable alkyllithium compound (*n*BuLi, *s*BuLi, or *t*BuLi). In this reaction [the so-called Directed *ortho* Metallation (D*o*M) reaction] the *ortho*-substituent acts as an *ortho*-directing group (*o*DG), which leads to the regioselective formation of the *ortho*-lithiated product.[3,4,18−20]

In our studies we frequently make use of *o*DG-arenes, in which the *o*DG is a CH(*Z*)NR_2 substituent, e.g., [(1-dimethylamino)methyl]benzene, 1,3-bis[(dimethylamino)methyl]benzene, and chiral derivatives (at the benzylic-C or -N centers) thereof. In several cases, we have observed that *ortho*-lithiation of these *o*DG-arenes with *n*BuLi in a 1:1 molar ratio did not proceed beyond 50% conversion, leaving unchanged *n*BuLi and *o*DG-arene, where subsequent quench experiments still indicated the presence of reactive butyl anions.[21,22] We believe that the unchanged BuLi becomes incorporated in mixed (*n*Bu/*o*DG-aryl)lithium aggregates and, in that way, becomes inaccessible for further reaction with free *o*DG-arene. Indeed, isolated examples of such mixed aggregates have been characterized.[23−26] Their existence is of importance, for example, when in situ-lithi-

[a] Debye Institute, Department of Metal-Mediated Synthesis, Utrecht University,
Padualaan 8, 3584 Utrecht, The Netherlands
[b] Bijvoet Center for Biomolecular Research, Crystal and Structural Chemistry, Utrecht University,
Padualaan 8, 3584 CH Utrecht, The Netherlands
Fax: (internat.) + 31-30-2523615
E-Mail g.vankoten@chem.uu.nl

ated *o*DG-arenes are used in subsequent transmetallation reactions; the presence of mixed (butyl/*o*DG-aryl)lithium aggregates, rather than quantitative lithiated *o*DG-arenes, will give rise to the formation of a mixture of butyl and *o*DG-aryl metal species instead of a pure *o*DG−aryl metal compound.

This paper descibes the factors that determine the formation and structural features of an enantiopure *o*DG-aryllithium compound, (*R*)-[$Li_4\{C_6H_4[CH(Me)NMe_2]\text{-}2\}_4$], and its racemic analog, *rac*-[$Li_4\{C_6H_4[CH(Me)NMe_2]\text{-}2\}_4$]. We will detail the synthesis of mixed (butyl/*o*DG-aryl)lithium aggregates in a future paper.

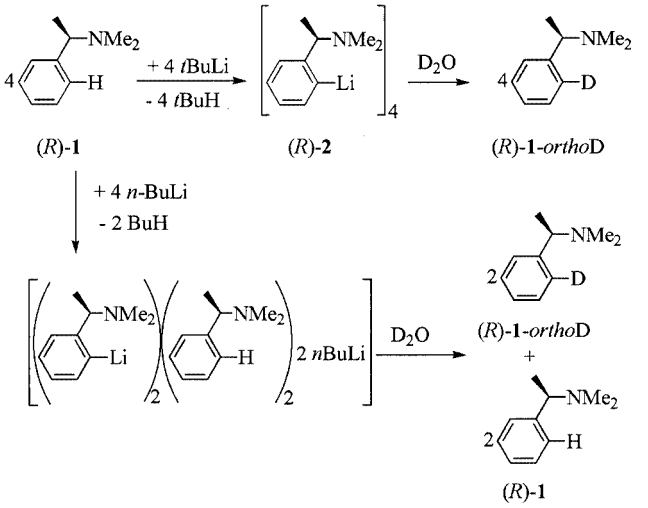

Scheme 1

Results and Discussion

Synthesis

Reaction of (*R*)-[1-(dimethylamino)ethyl]benzene [(*R*)-**1**] with *n*BuLi in a 1:1 molar ratio in diethyl ether at room temperature for 24 h, followed by quenching the reaction mixture with D_2O, afforded a 1:1 mixture of (*R*)-**1** and (*R*)-**1**-*ortho*D, which indicates that *ortho*-lithiation occurred to 50% completion (see Scheme 1). Based on this "chemical evidence," earlier we had proposed the formation of a species consisting of the *ortho*-lithiated arene, unchanged *n*BuLi, and the complexed parent *o*DG-arene in a 1:1:1 ratio.[21,22] The structural characterization of this species, i.e., [(*n*Bu)(*o*DG-aryl)Li_2(*o*DG-arene)], is still under investigation. In contrast, we found that the reaction of (*R*)-**1** with *t*BuLi instead of *n*BuLi[21] in pentane proceeded to completion and gave the pure *o*DG-aryllithium compound [$Li_4\{C_6H_4[CH(Me)NMe_2]\text{-}2\}_4$] [(*R*)-**2**], which was isolated as a white solid in an almost-quantitative yield (see Scheme 1). According to the same procedure, the racemic *o*DG-aryllithium compound *rac*-**2** was prepared starting from racemic [1-(dimethylamino)ethyl]benzene [*rac*-**1**].

The very different solubility of (*R*)-**2** and *rac*-**2** in hydrocarbon solvents, such as benzene and toluene, is striking. Whereas (*R*)-**2** has an almost infinite solubility in these solvents, making structural studies by NMR spectroscopic techniques in solution relatively easy, the corresponding racemic *rac*-**2** is essentially insoluble (< 1 mg/mL) in them. In this respect, it should be noted that the achiral analog of **2**, [$Li_4\{C_6H_4(CH_2NMe_2)\text{-}2\}_4$], which is isostructural with (*R*)-**2**, is also insoluble in hydrocarbon solvents.[27]

Structural Aspects of (*R*)- and *rac*-[$Li_4\{C_6H_4[CH(Me)NMe_2]\text{-}2\}_4$]

Crystals of (*R*)-**2** that were suitable for X-ray crystallography were obtained by treating (*R*)-**1** with *t*BuLi in pentane without stirring. Similar attempts to obtain suitable crystals of *rac*-**2** failed, invariably resulting in the formation of pure, but amorphous, *rac*-**2**.

The molecular geometry of (*R*)-**2** in the solid state reveals a tetranuclear aggregate in which the four lithium atoms are arranged in an almost-regular tetrahedron. Each of the aryl groups is bonded via C_{ipso} (five-coordinate) to one of the faces of the Li_4 tetrahedron, while the nitrogen atom of the *ortho*-amine substituent is coordinated to the apical position of a lithium atom, rendering this lithium atom four-coordinate. The overall structural geometry of (*R*)-**2** is de-

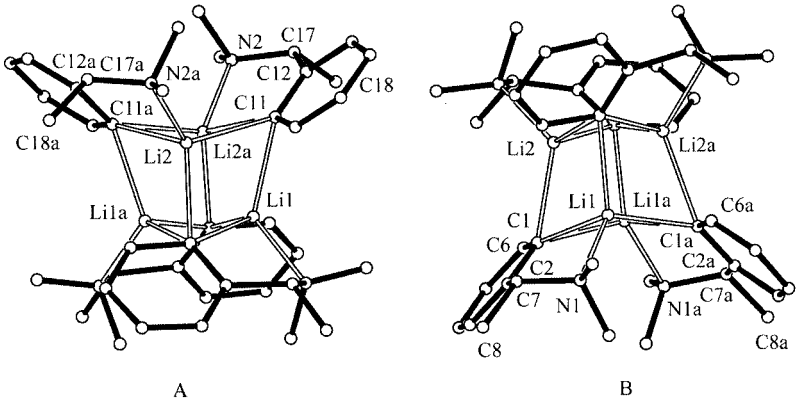

Figure 1. Ball-and-stick model of (*R*)-**2** in two different orientations; rotation (90°) of A along the *y* axis gives B; the $\mathbf{C}^2$ dimeric unit is clearly visible in the upper half of the Li_4 tetrahedron of A, while the $\mathbf{C}^1$ dimeric unit can be seen in the lower half of B (for $\mathbf{C}^1$ and $\mathbf{C}^2$, see Figure 4)

 © 2004 Wiley-VCH Verlag GmbH & Co. KGaA, Weinheim

picted in Figure 1. Relevant bond lengths and angles are given in Table 1.

Table 1. Selected bond lengths [Å] and torsion angles [°] for (*R*)-**2**

C1−Li1	2.250(3)	C11−Li2a	2.229(4)
C1−Li1a	2.309(3)	N1−Li1	2.040(3)
C1−Li2	2.341(3)	N2−Li2a	2.033(2)
C6···Li1a	2.414(3)	Li1−Li2	2.591(3)
C11−Li1	2.347(2)	Li1−Li1a	2.498(3)
C11−Li2	2.354(3)	Li1−Li2a	2.588(4)
		Li2−Li2a	2.551(4)
C1−C2−C7−C8	180.0(2)		
C11−C12−C17−C18	−96.5(2)	$a = 1 - x, -y, z$	

The basic structural features of (*R*)-**2** in the solid state closely resemble those reported earlier for $[Li_4\{C_6H_4[CH_2NMe_2]\text{-}2\}_4]$.[27] A useful way to describe the central $Li_4(C_{ipso})_4$ core in both structures is in terms of a distorted cube having alternating Li and C atoms, with the C atoms being the two-electron, four-center-bonded C_{ipso} atoms. The four *ortho*-amine-chelated aryl ligands span four edges of this cube, which can be realized in two different ways as shown in Figure 2.

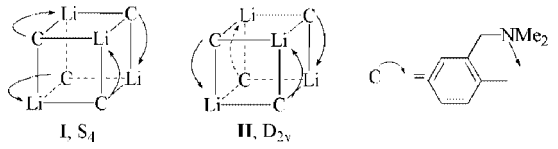

Figure 2. The two different ways in which the *C*,*N*-chelating ligands can span the edges of the Li_4C_4 cube

While the four *C*,*N*-ligands in **II** are symmetry-related by three perpendicular twofold axes, these four ligands in **I** are symmetry-related by a fourfold inversion axis. Precedents for both arrangements have been reported in the literature, e.g., $[Li_4\{C_6H_4[CH_2NMe_2]\text{-}2\}_4]$[27] and $[Li_4\{CH[Me]\text{-}CH_2CH_2OMe\}_4]$[28] have arrangement **I** while $[Li_4(CH_2CH_2CH_2NMe_2)_4]$[29,30] and $[Li_4(CH_2CH_2CH_2\text{-}OMe)_4]$[31] have arrangement **II**.

It is interesting to note that the central core of this type of Li_4 aggregate in both arrangements comprises an association of two dimeric units. Previously, we reported that the tetranuclear aggregate $[Li_4\{C_6H_4[CH_2NMe_2]\text{-}2\}_4]$ breaks down in THF into the corresponding THF-solvated dimers, although little structural data were available for such dimers at the time.[27,32] More recently, an elegant multinuclear NMR spectroscopy study was conducted using these dimers and related compounds in polar solvents, such as THF, diethyl ether, or a combination thereof. This study revealed that such dimers exist in polar, coordinating solvents as an equilibrium mixture of three geometrically different types of dimers: **A**, **B**, and **C**[33−36] (see Figure 3).

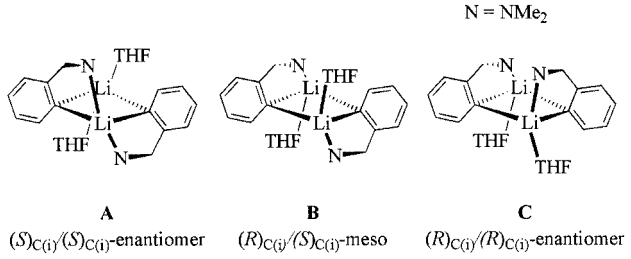

Figure 3. Three geometrically different isomers of $[Li_2(C_6H_4[CH_2NMe_2]\text{-}2)_2(THF)_2]$

In relation to the present study, it is important to note that dimers **A** and **C** are present as pairs of enantiomers, $(S)_{C(i)}$,$(S)_{C(i)}$ and $(R)_{C(i)}$,$(R)_{C(i)}$, respectively, while **B** is a *meso* form (see Figure 3). This situation arises because each of the bridging C_{ipso} atoms of the two-electron, three-center-bonded *ortho*-amino aryl groups in these aggragates has become a chiral center, labelled $(S)_{C(i)}$ or $(R)_{C(i)}$, which is a topic that has been discussed in detail earlier.[37,38] In fact, arrangements of types **I** and **II** found in the solid state comprise two associated dimers of type **C**. Furthermore, it was concluded that in solution the N−Li coordination is rigid on the NMR spectroscopic time scale.

A different situation arises when a second chiral center with a given configuration is added to the *C*,*N*-chelate ring (chiral labelling approach).[38] Figure 4 presents two different possibilities, $\mathbf{C}^1$ and $\mathbf{C}^2$, which are diastereoisomers, for a **C**-type dimer having a methyl-substituted benzylic carbon center with an *R* configuration [labelled $(R)_{C(b)}$], as is the case in (*R*)-**2**. For *rac*-**2**, a third type of dimer, i.e., $\mathbf{C}^3$ in Figure 4, should also be considered. The chiral benzylic carbon atoms have opposite configurations in this dimer. An interesting feature of this "racemic" dimer is the fact that the two *C*,*N*-chelate ligands are diastereotopic, i.e., they have different resonance patterns in NMR spectra.

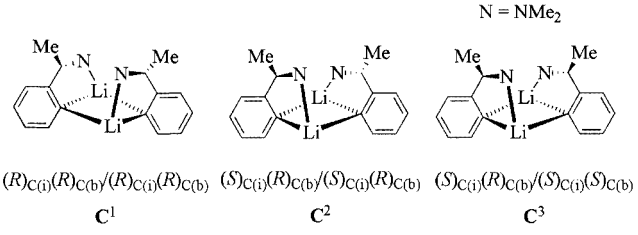

Figure 4. Three diastereoisomeric structures for a **C**-type dimer having a chiral center in the five-membered chelate-ring

These **C**-type diastereoisomers have different stereochemical features, in particular for the structural positioning of the benzylic methyl substituents in (*R*)-**2**. These substituents are pointing towards each other in $\mathbf{C}^1$, but in $\mathbf{C}^2$ they point in opposite directions. It is obvious that steric congestion in the latter type of dimer is lower, which most likely favors $\mathbf{C}^2$ over $\mathbf{C}^1$.

 © 2004 Wiley-VCH Verlag GmbH & Co. KGaA, Weinheim

At this point it is worth noting that, in the case of (*R*)-**2**, a type-**I** Li_4 arrangement (cf. Figure 2) can only be assembled by a combination of one $\mathbf{C}^1$ dimer and one $\mathbf{C}^2$ dimer, and consequently the Li_4 aggregate contains two diastereoisomeric (dimeric) parts. Combination of either two $\mathbf{C}^1$ or two $\mathbf{C}^2$ dimers always results in the formation of a type-**II** Li_4 arrangement. It is obvious that the latter will be the most favored one for steric reasons (vide supra).

The X-ray crystal structure of (*R*)-**2** reveals a type-**I** arrangement [all four benzylic carbon centers have (*R*) configuration]. For reasons outlined above, this tetranuclear aggregate contains two diastereoisomeric dimeric units, $\mathbf{C}^1$ and $\mathbf{C}^2$. This structural feature results in a rather-crowded situation for the methyl groups at the side of the cube that comprises the $\mathbf{C}^1$-type dimer. As a consequence of this crowding, the aryl groups are tilted in such a way that the aryl carbon atom next to C_{ipso}, i.e., C(6), lies in close proximity [2.418(3) Å] to one of the lithium atoms.

The ring pucker-conformations of the five-membered *C*,*N*-chelate rings in the $\mathbf{C}^1$ and $\mathbf{C}^2$ parts of (*R*)-**2** are distinctly different. In the $\mathbf{C}^2$-type dimeric part the α-methyl substituents are placed in the energetically favored antiperiplanar conformation with respect to the corresponding aryl ring [torsion angle −96.5(2)°]. In contrast, these α-methyl substituents in the $\mathbf{C}^1$-type dimeric part are orientated in-plane with respect to the corresponding aryl ring [torsion angle 180.0(2)°], which is an energetically less favorable conformer. It should be noted that in the latter situation, the opposite chelate ring puckering resulting in antiperiplanar-orientated methyl substituents would bring these methyl groups in very close proximity. Most probably the energetically less favored in-plane orientation in the solid state is compensated for by a sterically less congested situation.

Earlier studies[15,21] showed that (*R*)-**2** exists as tetrameric aggregates in non-coordinating solvents, such as benzene and toluene. The structure as observed for (*R*)-**2** in the solid state is most likely retained in these solvents, as can be concluded from the observed ^{1}H and ^{13}C NMR spectra recorded at various temperatures (see Table 2). Below −40 °C, in both ^{1}H and ^{13}C NMR spectra, two distinctly different resonance patterns are observed in a 1:1 ratio, which is in agreement with the situation observed in the solid state structure for (*R*)-**2**, which comprises two diastereoisomeric dimers, $\mathbf{C}^1$ and $\mathbf{C}^2$. Furthermore, this situation was confirmed by the observation of two resonances in a 1:1 ratio of intensities at δ = 0.09 and 0.14 ppm in the ^{6}Li NMR spectrum of (*R*)-**2**. In the ^{1}H NMR spectrum, a third resonance pattern is also present, although with lower intensity (ca. 10%), which could not be seen in the corresponding ^{13}C NMR spectrum because of the low signal-to-noise ratio. This additional resonance pattern displays an H(6) resonance at δ = 8.55 ppm, which is indicative of the presence of a C_{ipso}−Li bond, as well as an additional resonance of a benzylic hydrogen atom at δ = 3.05 ppm. We propose that the latter resonance pattern is the result of the presence of minor amounts of (*R*)-**2**, e.g., in the form of a type-**II** aggregate. It should be noted, based on symmetry considerations, that a type-**II** structure gives rise to only one resonance pattern for all four *ortho*-amine-chelated aryl groups. This observation could indicate that an equilibrium exists between the type-**I** and -**II** aggregates in solution, which in apolar solvents lies predominantly to the side of the type-**I** aggregate. Precedents for the existence of such an equilibrium have been documented for $[Li_4(CH_2CH_2CH_2NMe_2)_4]$,[29,30] which has a type-**II** structure in the solid state. ^{1}H, ^{13}C, and ^{7}Li NMR spectra at −40 °C in [D_8]toluene show, however, that in solution this compound exists as a 60:40 equilibrium mixture of type-**I** and type-**II** aggregates.[31]

Above −40 °C, the ^{1}H and ^{13}C NMR spectra of (*R*)-**2** indicate coalescence of the two resonance patterns, resulting in only one well-defined resonance pattern at 0 °C (see Table 2). Two resonances are still observed at this temperature for the diastereotopic NMe_2 methyl groups, which indicates that Li−N coordination is inert on the NMR spectroscopic time scale. A possible explanation for this observation is a process involving simultaneous scrambling of the bonding of the C_{ipso} atoms over the Li_3 faces of the Li_4 tetrahedron. In fact, the $\mathbf{C}^1$ dimer undergoes site exchange with the $\mathbf{C}^2$ dimer during such a process (cf. Figure 4). If such a process becomes fast on the NMR spectroscopic time scale it will result in magnetically equivalent aryl groups, without rendering the NMe_2 methyl groups enantiotopic. Finally, coalescence of the resonances of the diastereotopic NMe_2 methyl groups to a single resonance occurs at higher temperatures (> 40 °C), which points to a process involving Li−N dissociation/association that be-

Table 2. Relevant variable-temperature ^{1}H and ^{13}C NMR spectroscopic data for (*R*)-**2**[a]

T[a] [K]	δ (^{1}H) [ppm]				δ (^{13}C) [ppm]				
	NMe_2	α-Me	α-CH	*o*-H_{aryl}	NMe_2	α-Me	α-C	C1	C2
363	1.89	1.32	3.27	8.27	42.4	18.6	70.9	176.1	157.5
298	1.78 and 1.92	1.28	3.47	8.57	38.9 and 44.0	16.2	69.5	176.9	157.2
273	1.78 and 1.98	1.30 (br. s)	3.64 (br. s)	8.79 (br. s)	38.4 and 44.0	–[b]	68.3	175.9	157.2
233	–[c]	–	–	–	43.2 and 45.7	22.5	73.4	176.3	159.2
					35.6 and 42.9	8.4	64.4	183.1	156.9
193	1.38 and 1.67	1.17	3.28	9.01					
	1.93 and 2.30	1.93	4.83	9.01					

[a] All values are reported on the δ scale (ppm), relative to $SiMe_4$ as an external standard in [D_8]toluene as solvent. [b] Not observed. [c] Not measured.

 © 2004 Wiley-VCH Verlag GmbH & Co. KGaA, Weinheim

comes fast on the NMR spectroscopic time scale above this temperature.

As has been mentioned before, we were unable to obtain crystals of *rac*-**2** suitable for an X-ray crystallography. Moreover, the very limited solubility of *rac*-**2** in apolar solvents prevented ^{1}H and ^{13}C NMR spectroscopy studies to be undertaken in solution. For this reason we attempted to gain structural information about *rac*-**2** by comparison of the ^{13}C CP/MAS NMR spectra of *rac*-**2** and (*R*)-**2** (see Figure 5).

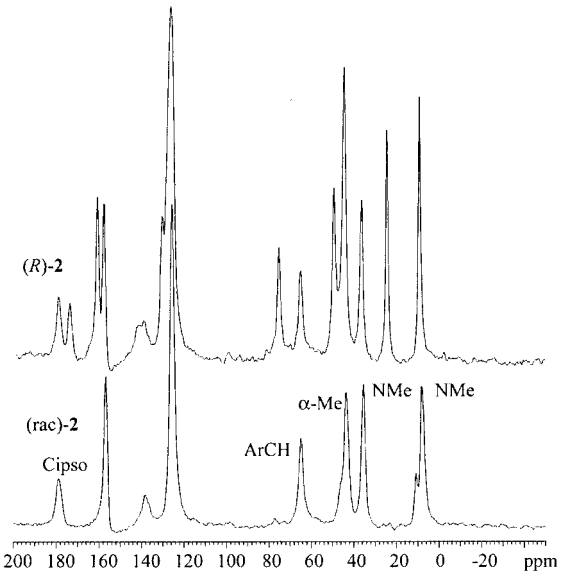

Figure 5. ^{13}C CP/MAS NMR spectra of (*R*)-**2** and *rac*-**2**

Two distinct resonance patterns are observed for (*R*)-**2** that are especially clear for C_{ipso}, C(6), the benzylic carbon atom, and the benzylic methyl substituent (see Figure 5). This spectrum is in full agreement with the structure observed for (*R*)-**2** in the solid state (two geometrically different **C**^{1} and **C**^{2} sites; vide supra). Interestingly, the ^{13}C CP/MAS NMR spectrum of *rac*-**2** shows only one distinct resonance pattern, which is similar to one of the patterns of (*R*)-**2**. An explanation for the relatively simple ^{13}C CP/MAS NMR spectrum of rac-**2** is that in the solid state rac-**2** exist as a type-**I** Li_4 aggregate comprising a combination of one **C**^{2}- and one **C**^{1}-type dimer. Furthermore, in the **C**^{1}-type dimeric unit of the Li_4 aggregate, the configuration of the two benzylic carbon centers is opposite to those in the **C**^{2}-type dimer. It should be noted that all four organic moieties in such an arrangement are symmetry-related by a fourfold inversion axis (vide supra). The alternative, i.e., a type-**II** aggregate in which the four organic moieties all have the same stereochemistry, is highly unlikely, because this arrangement would in fact represent a structure like that of (*R*)-**2** [or its enantiomer, (*S*)-**2**], which is known to have a type-**I** structure (vide supra). Finally, we note that a random distribution of *R* and *S* ligands over the Li_4 tetrahedron would give rise to very complicated spectra as a result of the formation of a variety of diastereoisomeric aggregates.

Further studies are underway directed to determine the relative thermodynamic and kinetic stabilities of the tetranuclear assemblies of (*R*)-**2** and *rac*-**2**. In particular, we expect that these species have different rates for the tetramer−dimer equilibria in polar, coordinating solvents (THF, Et_2O), as well as different reactivities for the formation of mixed aggregates with other alkyl- or aryllithium species or even lithium salts.[24−26]

Experimental Section

General Remarks: All experiments were carried out under a dry, oxygen-free, nitrogen atmosphere, using standard Schlenk techniques. Solvents were dried and distilled from Na/benzophenone prior to use. The *n*BuLi (1.6 M in hexane) and *t*BuLi (1.5 M in pentane) solutions were ordered in 10-g nitrogen sure-sealed bottles and used as received after determination of the exact concentration by titration with 1,10-phenantroline in 2-butanol/*m*-xylene (1 M). ^{1}H, ^{13}C, ^{6}Li, and ^{13}C CP/MAS NMR NMR spectra were recorded on a Varian 300 MHz spectrometer at ambient temperature, unless stated otherwise. Chemical shifts (δ) are given in ppm relative to $SiMe_4$ as an external standard. The ^{6}Li NMR spectra were referenced to LiCl in D_2O (1.0 M) as an external standard. Elemental analyses were obtained from Dornis und Kolbe Mikroanalytisches Laboratorium, Mülheim a.d. Ruhr, Germany.

Synthesis of [Li{(*R*)-C_6H_4[CH(Me)NMe_2]-2}]$_4$ [(*R*)-2]: This species was prepared according to a published procedure,[21] starting from (*R*)-$C_6H_5CH(Me)NMe_2$ and *t*BuLi. Crystals suitable for X-ray crystallography were obtained by performing the reaction without stirring. When (*S*)-$C_6H_5CH(Me)NMe_2$ is subjected to the same lithiation reaction, the related analog, (*S*)-**1**, was obtained in a straightforward manner. ^{1}H NMR (C_6D_6, 300.105 MHz, 298 K): δ = 1.13 [d, ^3J = 6.71 Hz, 3 H, CH(*Me*)], 1.62 (br. s, 3 H, N*Me*$_2$), 1.72 (br. s, 3 H, N*Me*$_2$), 3.33 [br. s, 1 H, C*H*(Me)], 7.05 [d, ^3J = 7.32 Hz, 1 H, ArH(*3*)], 7.20 [dt, 1 H, ^3J = 7.03 Hz, ArH(*4*)], 7.26 [t, ^3J = 7.03 Hz, 1 H, ArH(*5*)], 8.47 [bd, 1 H, ArH(*6*)] ppm. ^{13}C NMR ([D$_8$]toluene, 75.469 MHz, 298 K): δ = 17.5 (br. s, C*C*H$_3$), 38.9, 44.0 (br. s, N*Me*$_2$), 69.4 (br. s, Ar*C*H), 124.6, 125.2, 125.5, 140.9 [Ar(*3,4,5,6*)], 157.2, 175.9 [Ar(*1,2*) quaternary] ppm. ^{6}Li NMR ([D$_8$]toluene, 44.165 MHz, 218 K): δ = 0.09 and 0.14 ppm. $C_{40}H_{56}N_4Li_4$ (600.5): calcd. C 77.41, H 9.09, N 9.03%; found C 77.28, H 8.93, N 9.01%.

The *rac*-**2** species was prepared in a similar way starting from *rac*-$C_6H_5CH(Me)NMe_2$.

X-ray Crystal Structure Analyses of (*R*)-2: Pertinent data for the structure determinations are collected in Table 3. X-ray data were collected on a Nonius CAD-4T diffractometer. The data set was measured at 150 K, using graphite-monochromated Mo-*K*α radiation (λ = 0.71073 Å) from a rotating anode source. Accurate unit cell parameters and an orientation matrix were determined by least-squares fitting of the setting angles of 25 well-centered reflections.[39] The structure was solved by direct methods using SHELXS-86.[40] Refinement on F^2 was performed with SHELXL-97.[41] Hydrogen atoms were included in the refinement on calculated positions riding on their carrier atoms. The non-hydrogen atoms of the structure were refined with anisotropic displacement parameters. The hydrogen atoms were refined with a fixed isotropic displacement parameter related by a constant factor to the value of the equivalent isotropic displacement parameter of their carrier atoms. Because of the absence of strong anomalous scatters, the

 © 2004 Wiley-VCH Verlag GmbH & Co. KGaA, Weinheim

absolute configuration could not be determined experimentally. The absolute configuration was therefore assigned in accordance with the known configuration of the asymmetric carbon atoms of the starting compound. Geometrical calculations and illustrations were performed with PLATON;[42] all calculations were performed on a DEC Alpha 255 station. CCDC-212315 contains the supplementary crystallographic data for this paper. These data can be obtained free of charge at www.ccdc.cam.ac.uk/conts/retrieving.html [or from the Cambridge Crystallographic Data Centre, 12 Union Road, Cambridge CB2 1EZ, UK; Fax: (internat.) + 44-1223/336-033; E-mail: deposit@ccdc.cam.ac.uk].

Table 3. Crystallographic data for the crystal structure determination of (*R*)-**2**

Compound	(*R*)-**2**
Crystal Data	
Formula	$C_{40}H_{56}Li_4N_4$
Mol. Weight	620.65
Crystal System	orthorhombic
Space group	$P2_12_12$ (No. 18)
a [Å]	11.8653(8)
b [Å]	15.6471(11)
c [Å]	10.0929(8)
V [Å^3]	1873.8(3)
$D_{calcd.}$ [g cm^{-3}]	1.100
Z	2
F(000)	672
μ [mm^{-1}] Mo-K_α	0.062
Crystal color	yellow
Crystal size [mm]	0.6 × 0.6 × 0.6
Data Collection	
θ_{min}, θ_{max} [deg]	1.3, 27.5
Temperature [K]	150
Data set	−15:15, −20:0, −13:0
Total data	4911
Total unique data	2241 [R_{int} = 0.035]
Refinement	
No. of parameters	223
Final R_1[a]	0.0379 [2457 $I > 2\sigma(I)$]
Final wR_2[b]	0.101
Goodness of Fit	1.043
w^{-1}[c]	$\sigma^2(F^2) + (0.0537P)^2 + 0.25P$
$(\Delta/\sigma)_{max}$, $(\Delta/\sigma)_{av}$	< 0.001, < 0.001
$\Delta\rho_{min}$, $\Delta\rho^{max}$ [e A^{-3}]	−0.15, 0.21

[a] $R_1 = \Sigma||F_o| - |F_c||/\Sigma|F_o|$. [b] $wR_2 = \Sigma[w(F_o^2 - F_c^2)^2/\Sigma[w(F_o^2)^2]]^{1/2}$. [c] $P = \mathrm{Max}(F_o^2,0) + 2F_c^2)/3$.

Acknowledgments

This work was supported in part (A.L.S.) by The Netherlands Foundation for Chemical Sciences (CW) with financial aid from the Netherlands Organization for Scientific Research (NWO). Dr. J. Boersma is thanked for critically reading this manuscript.

[1] B. J. Wakefield, *The Chemistry of Organolithium Compounds*; Pergamon Press, New York, **1974**.
[2] J. L. Wardell, *Comprehensive Organometallic Chemistry*; Pergamon Press, New York, **1982**; vol. 1, chapter 2.
[3] H. W. Gschwend, H. R. Roderiguez, *Org. React.* **1979**, *26*, 1−360.
[4] V. Snieckus, *Chem. Rev.* **1990**, *90*, 879−933 and references cited therein.
[5] M. Albrecht, G. van Koten, *Angew. Chem. Int. Ed.* **2001**, *40*, 3750−3781; *Angew. Chem.* **2001**, *113*, 3866−3898.
[6] G. van Koten, J. G. Noltes, *J. Chem. Soc., Chem. Commun.* **1972**, 940−941.
[7] G. van Koten, J. T. B. H. Jastrzebski, *Tetrahedron* **1989**, *45*, 569−578.
[8] N. P. Lorenzen, E. Weiss, *Angew. Chem. Int. Ed. Engl.* **1990**, *29*, 300−302; *Angew. Chem.* **1990**, *102*, 322−324.
[9] C. M. P. Kronenburg, J. T. B. H. Jastrzebski, A. L. Spek, G. van Koten, *J. Am. Chem. Soc.* **1998**, *120*, 9688−9689.
[10] E. Rijnberg, J. T. B. H. Jastrzebski, J. Boersma, H. Kooijman, N. Veldman, A. L. Spek, G. van Koten, *Organometallics* **1997**, *16*, 2239−2245.
[11] G. van Koten, S. L. James, J. T. B. H. Jastrzebski, *Comprehensive Organometallic Chemistry*; Pergamon Press, New York, **1995**; vol. 3, chapter 2.
[12] W. M. Setzer, P. v. R. Schleyer, *Adv. Organomet. Chem.* **1985**, *24*, 353−451.
[13] D. Seebach, R. Hässig, J. Gabriel, *Helv. Chim. Acta* **1983**, *66*, 308−337.
[14] W. Bauer, W. R. Winchester, P. v. R. Schleyer, *Organometallics* **1987**, *6*, 2371−2379.
[15] E. Wehman, J. T. B. H. Jastrzebski, J.-M. Ernsting, D. M. Grove, G. van Koten, *J. Organomet. Chem.* **1988**, *353*, 133−143.
[16] R. J. Wehmschulte, P. P. Power, *J. Am. Chem. Soc.* **1997**, *119*, 2847−2852.
[17] H. J. Reich, D. P. Green, M. A. Medina, W. S. Goldenberg, B. Ö. Gudmundsson, R. R. Dykstra, N. H. Phillips, *J. Am. Chem. Soc.* **1998**, *120*, 7201−7210.
[18] H. Gilman, R. L. Bebb, *J. Am. Chem. Soc.* **1939**, *61*, 109−112.
[19] G. Wittig, G. Fuhrman, *Ber. Dtsch. Chem. Ges.* **1940**, *73*, 1197−1218.
[20] H. Gilman, J. W. Morton, *Org. React. (N. Y.)* **1954**, *8*, 258−304.
[21] G. van Koten, J. T. B. H. Jastrzebski, *Tetrahedron* **1989**, *45*, 569−578.
[22] G. van Koten, J. T. B. H. Jastrzebski, C. H. Stam, C. Brevard, *Biological and Inorganic Copper Chemistry* (Eds.: K. D. Karlin, J. Zubieta), Adenine Press, **1985**, pp. 267−285.
[23] K. Ruhlandt-Senge, J. J. Ellinson, R. J. Wehmschulte, F. Pauer, P. P. Power, *J. Am. Chem. Soc.* **1993**, *115*, 11353−11357.
[24] J. G. Donkervoort, J. L. Vicario, E. Rijnberg, J. T. B. H. Jastrzebski, H. Kooijman, A. L. Spek, G. van Koten, *J. Organomet. Chem.* **1998**, *550*, 463−467.
[25] P. Wijkens, E. M. van Koten, M. D. Janssen, J. T. B. H. Jastrzebski, A. L. Spek, G. van Koten, *Angew. Chem. Int. Ed. Engl.* **1995**, *34*, 219−222; *Angew. Chem.* **1995**, *107*, 239−242.
[26] P. Wijkens, J. T. B. H. Jastrzebski, N. Veldman, A. L. Spek, G. van Koten, *Chem. Commun.* **1997**, 2143−2144.
[27] J. T. B. H. Jastrzebski, G. van Koten, M. Konijn, C. H. Stam, *J. Am. Chem. Soc.* **1982**, *104*, 5490−5492.
[28] G. W. Klumpp, P. J. A. Geurink, A. L. Spek, A. J. M. Duisenberg, *J. Chem. Soc., Chem. Commun.* **1983**, 814−816.
[29] G. W. Klumpp, M. Vos, F. J. J. de Kanter, C. Slob, H. Krabbendam, A. L. Spek, *J. Am. Chem. Soc.* **1985**, *107*, 8292−8294.
[30] K. S. Lee, P. G. Williard, J. W. Suggs, *J. Organomet. Chem.* **1986**, *299*, 311−317.
[31] G. W. Klumpp, P. J. A. Geurink, N. J. R. van Eikema Hommes, F. J. J. de Kanter, M. Vos, A. L. Spek, *Recl. Trav. Chim. Pays-Bas* **1986**, *105*, 398−403.
[32] E. Wehman, J. T. B. H. Jastrzebski, J.-M. Ernsting, D. M. Grove, G. van Koten, *J. Organomet. Chem.* **1988**, *353*, 145−155.
[33] H. J. Reich, B. Ö. Gudmundsson, *J. Am. Chem. Soc.* **1996**, *118*, 6074−6075.
[34] H. J. Reich, W. S. Goldenberg, B. Ö. Gudmundsson, A. W.

 © 2004 Wiley-VCH Verlag GmbH & Co. KGaA, Weinheim

Sanders, K. J. Kulicke, K. Simon, I. A. Guzei, *J. Am. Chem. Soc.* **2001**, *123*, 8067−8079.
[35] H. J. Reich, W. S. Goldenberg, A. W. Sanders, C. C. Tzschucke, *Org. Lett.* **2001**, *3*, 33−36.
[36] H. J. Reich, W. S. Goldenberg, A. W. Sanders, K. L. Jantzi, C. C. Tzschucke, *J. Am. Chem. Soc.* **2003**, *125*, 3509−3521.
[37] The configuration of the bridging C_{ipso} center in the rotamer having the aryl plane perpendicular to the Li−Li vector is determined by the priority of the atoms connected to C_{ipso} in the *C*,*N*-chelate ring, viewing in the direction of the second Li atom.
[38] G. van Koten, J. G. Noltes, *J. Am. Chem. Soc.* **1979**, *101*, 6593−6599.
[39] J. L de Boer, A. J. M. Duisenberg, *Acta Crystallogr., Sect. A* **1984**, *40*, C-410.
[40] G. M. Sheldrick, *SHELXS-86 Program for crystal structure determination*, University of Göttingen, Germany, **1986**.
[41] G. M. Sheldrick, *SHELXL-97 Program for crystal structure refinement*, University of Göttingen, Germany, **1997**.
[42] A. L. Spek, *J. Appl. Cryst.* **2003**, *36*, 7−13.

Received September 1, 2003

 © 2004 Wiley-VCH Verlag GmbH & Co. KGaA, Weinheim